

1
2
3 *Infrasound observations of sprites associated with winter thunderstorms in the eastern*
4
5 *Mediterranean*
6
7

8 David Applbaum¹, Gil Averbuch¹, Colin Price¹, Yoav Yair², Yochai Ben-Horin³
9

10
11 ¹ Tel Aviv University, Ramat Aviv, Israel
12

13 ² Interdisciplinary Center (IDC) Herzliya, Herzliya, Israel
14

15 ³ Soreq Nuclear Research Center, Israel
16
17

18 **Abstract**
19

20
21 Sprites are transient luminous events (TLEs) that occur at mesospheric altitudes between 50 and
22
23 90 km. They last up to several milliseconds, and are caused mostly by positive lightning
24
25 discharges from the thunderstorm cells below. Infrasound from sprites was first observed in
26
27 detail a decade ago by a team from the French Atomic Energy Commission (CEA), as part of a
28
29 renewed international interest in infrasound measurements brought about by the Comprehensive
30
31 Nuclear Test Ban Treaty (CTBT) [1]. They used optical images of sprites obtained during the
32
33 EuroSprite observation campaign in order to form the temporal and azimuthal basis necessary for
34
35 searching for the infrasound signatures from these events, which appear as unique “chirp” or
36
37 “inverted chirp” signatures depending on the sprite’s distance from the infrasound array. In this
38
39 paper we follow this methodology to see if the nascent Israeli infrasound arrays can detect these
40
41 signals from sprites in the Eastern Mediterranean, for which there are nearly 8 years of winter-
42
43 time optical observations. We calculated the expected arrival time of the infrasound from
44
45 optically observed sprites, and then used a basic ray-tracing method in order to confirm that we
46
47 were in fact able to observe several of these sprites, at various distances, exhibiting both “chirp”
48
49
50
51
52
53
54
55
56

57
58
59 and “inverted chirp” signals. We then compared these observations with observations of
60 lightning activity made by the World Wide Lightning Location Network (WWLLN).
61
62

63 64 **Introduction**

65
66
67 Sprites are transient luminous events (TLEs) that occur at mesospheric altitudes between 50 and
68 90 km. They last up to several tens of milliseconds, and are triggered by positive lightning
69 discharges from the storm cells below. They are usually described as a group of visible columns,
70 sometimes with branching features that make them appear jelly-fish or carrot-like, and many
71 images have been taken of them all over the world [2]–[4]. Israel is an ideal place to observe
72 these phenomena, owing to the fact that thunderstorms in the eastern Mediterranean occur in
73 winter-time, when the nights are longest, and because the sea provides few viewing obstructions
74 [5]. This allows for a much greater chance of imaging the sprites, which are virtually impossible
75 to see when there is any daylight at all [6].
76
77
78
79
80
81
82
83
84
85

86
87 That sprites produce detectable pressure waves was first theorized by Bedard et al [7]. Later,
88 Liszka [8] observed signals in his infrasound data that he attributed to sprites. These were
89 pressure pulses of between 0.01 and 0.1 Pa, lasting several tens of seconds, and with lower
90 frequencies arriving first. He described these changes in frequency content with time as
91 “chirps.” Farges et al [1] confirmed this with extensive infrasound observations of optically-
92 imaged sprites, observing these chirps originating from sprites occurring about 400 km away
93 from their infrasound array. The chirps are explained by a combination of the sprite’s size and
94 location. Sprites at 400 km produce infrasound that reflects off of the atmosphere at higher
95 altitude—where the effective sound speed increases with the increase in temperature—before
96 traveling to the infrasound arrays. During this reflection, the waves are damped slightly, and
97 there is attenuation of higher frequencies that increases with altitude. Therefore, signals coming
98
99
100
101
102
103
104
105
106
107
108
109
110
111
112

113
114
115 from the higher-altitude parts of sprites (~ 80 km) arrive depleted in their upper frequency
116
117 ranges. Signals from the lower altitude parts of sprites (~ 50 km) are reflected from lower
118
119 altitudes, making their frequency spectrum more complete and their arrival slightly delayed,
120
121 resulting in an infrasound signal that begins with lower frequencies and ends with all
122
123 frequencies, including the higher ones [1], [9], [10]. Depending on the size of the sprite and the
124
125 distance to the receiver, these “higher” frequencies can be anything from 2 to 10 Hz, with the
126
127 “lower” frequencies being less than 2 Hz. Liszka and Hobara [8] then further studied this
128
129 phenomenon through an automatic search for these signals within ten years of their data.
130
131

132
133 Upon further review of the 2005 study, Farges and Blanc [10] reported seeing even more signals
134
135 of appropriate length and frequency content, only this time, the high frequencies arrived before
136
137 the low frequencies, in what they called “inverted chirps.” This was explained intuitively by de
138
139 Larquier and Pasko that same year. Because of the closer distances, the infrasound interceptions
140
141 are direct, and the closer, lower altitude signals arrive before the farther, higher altitude (and
142
143 higher-frequency-depleted) ones [11].
144

145
146 In this paper, we will show our infrasound interceptions of both a “chirp” from a distant sprite
147
148 and an “inverted chirp” from a closer range sprite, which occurred in winter thunderstorms over
149
150 the eastern Mediterranean Sea.
151

152 **Equipment**

153
154
155 In 2003 the ILAN (Imaging of Lightning and Nocturnal flashes) project was started, named after
156
157 the late Israeli astronaut Ilan Ramon, with the mission of imaging and cataloguing as many
158
159 eastern Mediterranean sprites as possible. The ILAN team set up two observation sites, with two
160
161 panchromatic CCD cameras at each site: one at Tel Aviv University (32.5N, 34.5E), with a view
162
163
164
165
166
167
168

169
170
171 of sprites occurring up to 400 km off the Mediterranean coast, and one at the Wise Observatory
172
173 in Mizpe Ramon (30.6N, 34.76E), better at capturing sprites closer to the coast and above
174
175 northern Israel . The systems were equipped with UFO-capture software in order to isolate
176
177 events automatically, therefore allowing the team to delete event-free data and avoid the need for
178
179 data compression. The pan-and-tilt unit (PTU) recorded the azimuth with 0.1 degree accuracy.
180
181 The field of view (FOV) of the primary camera was 14 degrees in the horizontal direction, and
182
183 10.5 degrees vertical [2], [12].
184
185

186
187 The Israel Infrasound Network consists of two arrays of MB2000 micro-barometers attached to
188
189 Quanterra Q330 digitizers. One array, with four elements, is in the Negev desert, near the town
190
191 of Dimona; the other, with five elements, is near the northern town of Meron, close to the border
192
193 with Lebanon. The arrays have been functioning nearly continuously since 2011. The Meron
194
195 array has a much smaller aperture (1km as compared with nearly 5km for the Dimona array),
196
197 making it much more appropriate for studying signals with wavelengths corresponding to the
198
199 frequency ranges of sprites, and thus, this is the array we used for this study [13].
200
201

202
203 The World Wide Lightning Location Network, or WWLLN, is a worldwide network of about 70
204
205 very low frequency - VLF (3-30 kHz) detectors [14], organized by the University of Washington
206
207 in collaboration with many other universities. WWLLN works by using ground-based detectors
208
209 to intercept the VLF emissions from lightning known as sferics, localizing them using the time of
210
211 group arrival (TOGA) technique. It takes advantage of the fact that these waves travel thousands
212
213 of kilometers in the Earth-ionosphere waveguide without significant attenuation [15]. As with
214
215 infrasound, WWLLN only sees a representative fraction of the total lightning activity, about 11%
216
217 on average [16], though the location error of these detections is within 2.9 km, on average [17].
218
219
220
221
222
223
224

225
226
227 **Methods**
228
229

230 We received the complete list of optical sprite observations from the ILAN science team. These
231 data include time, azimuth, elevation, distance, physical description (for example, “carrot” or
232 “column”), and number of elements (meaning the number of optically distinct structures)[18].
233
234

235
236
237 Infrasound waveform analysis was performed using Progressive Multi-Channel Correlation
238 (PMCC) [19]. In order to determine which time periods to analyze in the infrasound data, we
239 calculated arrival windows, by determining how long the infrasound transit time would be if it
240 traveled only at the lowest and highest possible sound speeds it could encounter, taken to be 250
241 m/s at 90km and 340 m/s at sea level. Subtracting the two gave us a window of up to 10 minutes
242 (and in most cases much less) during which the infrasound wave from the sprite could have
243 arrived at the micro-barometer array. Because each sprite infrasound signal is tens of seconds
244 long, we expected it to be well isolated in our arrival window. Indeed, in almost every case
245 where an infrasound signal appeared, only one signal of appropriate length was visible in the
246 arrival window.
247
248
249
250
251
252
253
254
255
256
257
258

259 We repeated this process for all ~330 sprites observed by the ILAN science team in the years
260 2011-2013. In most cases, we were not able to see any signals at all in the infrasound. This we
261 attributed to the fact that most sprites observed were optically small, listed as having only a
262 single discernable element. While the average sprite deposits a few to tens of MJ into the
263 atmosphere [20], a sprite must deposit hundreds of MJ into the atmosphere in order to produce
264 even a 0.1 Pa pressure wave observable at a distance of hundreds of km [21] [22]. This means
265 that the likelihood of any individually-imaged sprite being detected in infrasound is not very high
266 [21]. However, we were able to observe the majority of the sprites with more than 8 observed
267 structural elements, which themselves were just 5% of the sprites observed by the ILAN team.
268
269
270
271
272
273
274
275
276
277
278
279
280

281
 282
 283 In cases where more than one sprite occurred in close enough succession so as to cause
 284
 285 infrasound arrival windows to overlap, we used ray tracing to determine which specific
 286
 287 photographed sprite caused the observed infrasound signal. We used a 3D ray tracing model
 288
 289 based on a modified Eikonal for a moving medium [23] solved by using the Hamiltonian
 290
 291 representation of the system, using the short distance of the sprites from the observation points in
 292
 293 Israel in order to neglect the curvature of the Earth [24]. This model requires two atmospheric
 294
 295 parameters: the speed of sound profile and the wind profile. We used local averaged profiles for
 296
 297 the winter time, consistent with other infrasound modeling studies done in the same geographical
 298
 299 region [25]. Local radiosonde measurements enabled us to update the first 20 Km of both speed
 300
 301 of sound and wind profiles.
 302
 303

$$304 \mathcal{H}(q_i, p_i) = \frac{1}{2} [p_i^2 - u(q_i)^2 (1 - p_i v(q_i))^2]$$

305
 306 p_i is the slowness vector, q_i is the position in space and $u = \frac{1}{c}$. The differential equations for the
 307
 308 slowness vector, position and propagation time are:
 309
 310
 311
 312
 313
 314
 315
 316
 317

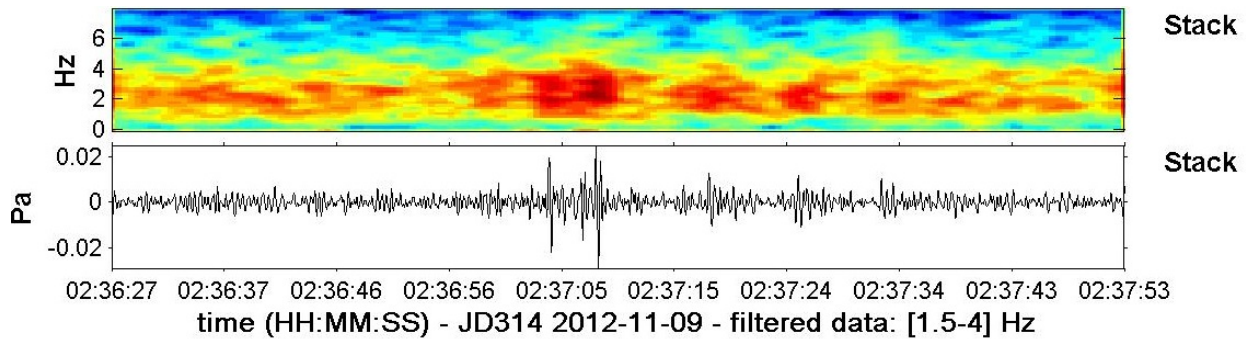
$$318 \frac{dq_i}{d\tau} = \frac{\partial \mathcal{H}}{\partial p_i} = p_i + u^2 (1 - p_i v_i) v_i$$

$$319 \frac{dp_i}{d\tau} = - \frac{\partial \mathcal{H}}{\partial q_i} = u^2 (1 - p_i v_i) p_i \frac{\partial v_l}{\partial q_l} - \frac{1}{2} (1 - p_i v_i)^2 \frac{\partial u^2}{\partial q_i}$$

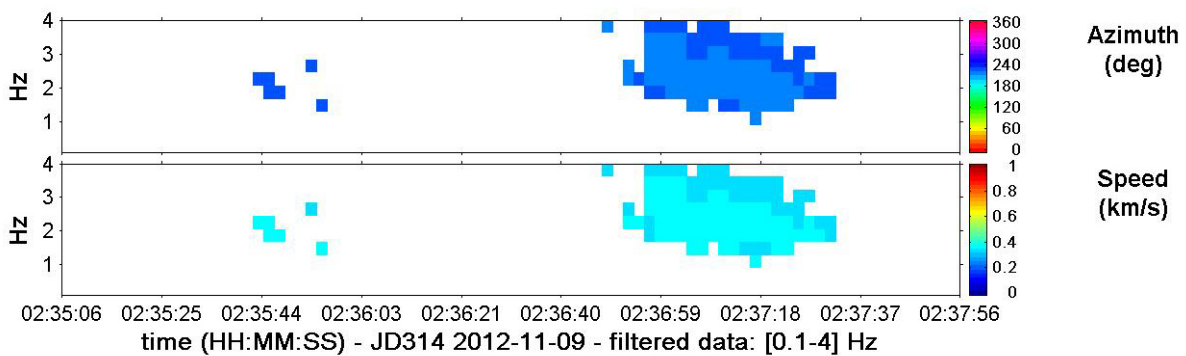
$$320 \frac{dT}{d\tau} = p_i \frac{\partial \mathcal{H}}{\partial p_i}$$

321 Results

337
 338
 339 An example of a sprite from the ILAN database that we were able to observe occurred on 9
 340
 341 November, 2012 at 02:25:49 UTC. We received the infrasound pressure pulse at approximately
 342
 343 02:36:50 UTC at the Meron station. Figure 1 shows the spectrum of this signal, and the acoustic
 344
 345 waves incident on the micro-barometers have been stacked so that the pressure signal is more
 346
 347 clearly visible. Figure 2 shows PMCC analysis of the intercepted waveform. Visible is the
 348
 349 “inverted chirp” signal typical of sprites observed from distances of less than 200 km [10], in
 350
 351 which the end of the signal arrives depleted of its higher frequencies.
 352
 353
 354



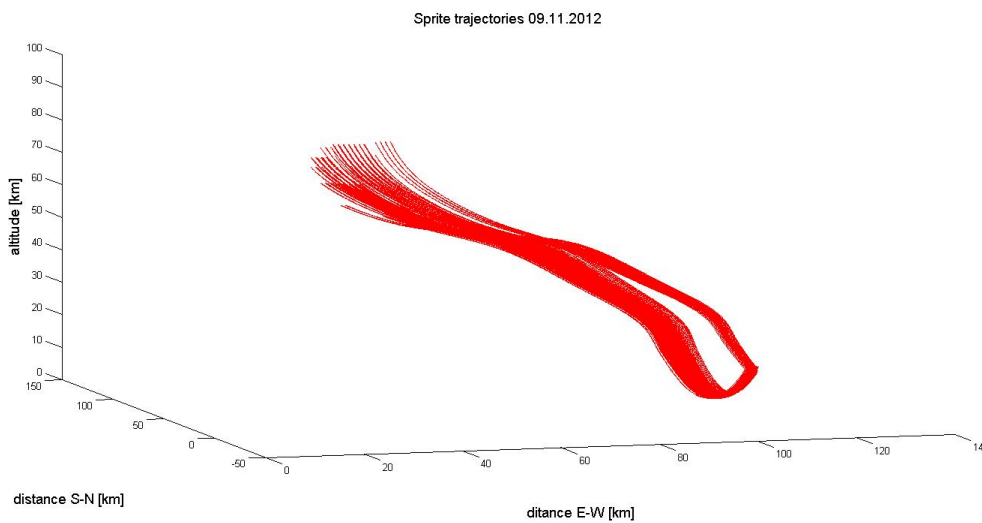
367 Figure 1: Pressure spectrum and stacked pressure pulse of the sprite signal



385 Figure 2: PMCC waveform analysis of a sprite on 9 November, 2012

386 This signal lay in the arrival windows of five different sprites in the optical database, all
 387
 388 occurring within a few minutes of each other and all co-located approximately 190 km to the
 389
 390
 391
 392

393 southwest of the Meron infrasound array, in agreement with the approximately 220-degree back-
394 azimuth of the infrasound signal (Figure 4). We simulated the different possible arrival times
395 using the ray tracing method described above, and determined that the sprite we intercepted was
396 the one imaged by the Mizpe Ramon camera at 02:25:49. Although a visual image of this sprite
397 was not saved in the database, it was described by the observer as having 10 elements, the most
398 of any of the candidates. As seen in Figure 3, the highest altitude (70-80 km) rays were directly
399 incident upon the infrasound detectors, whereas the lower altitude rays (65-70) made a shallower
400 yet faster path, spending more time at lower altitude (where the sound speed is higher) and
401 reflecting off the ground before arriving at the detector. The highest density of initial ray
402 positions came from the area between the sprite's optically-registered location and the back-
403 azimuth of the infrasound data (Figure 4). This slight difference between the actual back-
404 azimuth and the PMCC-calculated infrasound back-azimuth is likely due to local winds.
405
406
407
408
409
410
411
412
413
414
415
416
417
418
419
420
421



422
423
424
425
426
427
428
429
430
431
432
433
434
435
436
437
438 Figure 3: Ray tracing simulation for the sprite in Figure 1
439
440
441
442
443
444
445
446
447
448

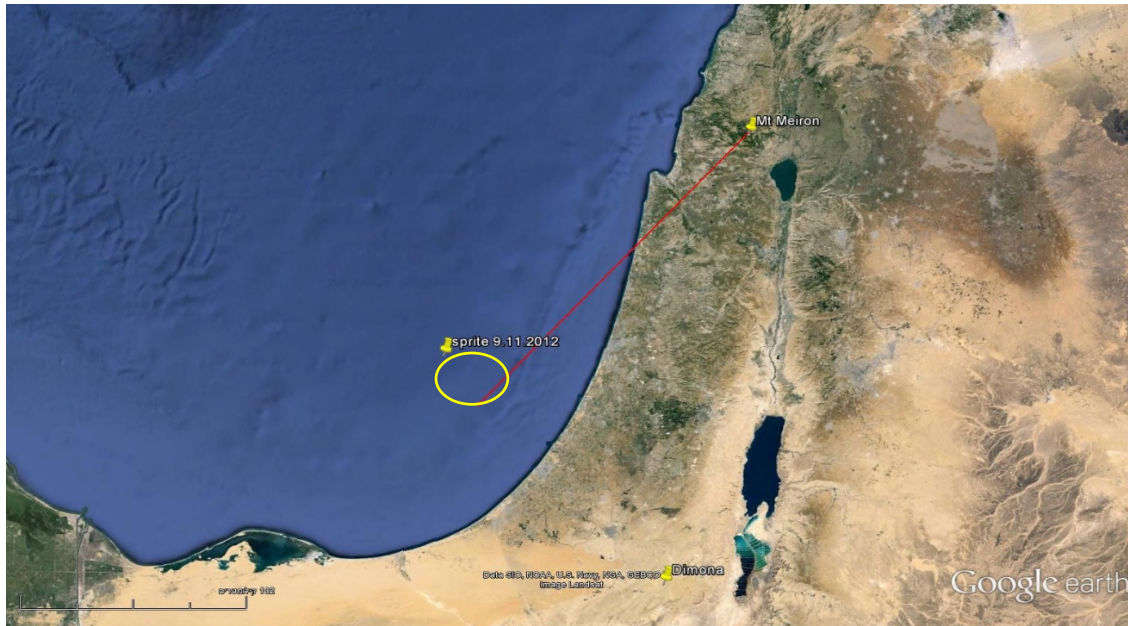


Figure 4: Oval showing the highest density area for initial ray position for the infrasound signal detected in Figure 1

When comparing this detection with WWLLN detections from the same period (Figure 5), it is readily apparent that there was lightning activity detected at the correct time from the area predicted by the infrasound interception and ray tracing model. However, as previously discussed, since neither WWLLN nor ILAN record 100% of lightning, it is difficult to say whether any of these individual flashes is associated with the specific sprite detected.

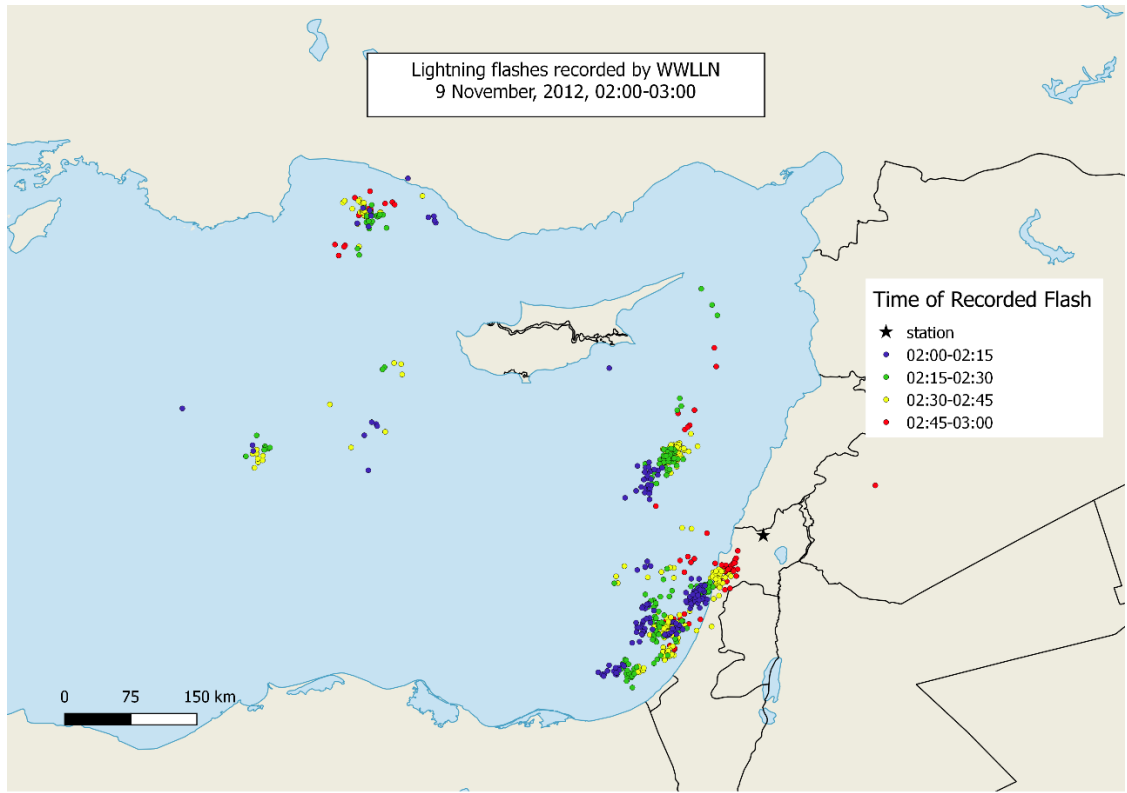


Figure 5: WWLLN Lightning Flash detections from the same time period as when the sprite was observed. There was lightning detected from the vicinity of the area predicted by the infrasound interception and ray tracing model. The sprite occurred during the time interval pictured in yellow.

We received another sprite-like infrasound signature on 6 January, 2011, at approximately 20:36:00, which we compared with one of four sprites imaged by ILAN between 16 and 20 minutes prior. The database entries are below in Table 1, and include the photographs, which in this case were saved.

561
562
563
564
565
566
567
568
569
570
571
572
573
574
575
576
577
578
579
580
581
582
583
584
585
586
587
588
589
590
591
592
593
594
595
596
597
598
599
600
601
602
603
604
605
606
607
608
609
610
611
612
613
614
615
616

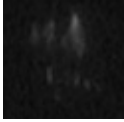
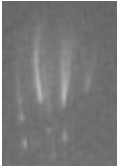
Time (UTC)	Sprite
20:16:18:040	
20:16:18:900	
20:19:05:245	
20:19:05:240	

Table 1: database entries for candidate sprites

The ILAN camera in Tel Aviv put these sprites about 380 km to the northwest of the Meron infrasound array, off the coast of Cyprus, in agreement with the approximately 285-degree back azimuth of the infrasound signal. Figure 7 shows the signal spectrum and the pressure pulse from all of the stacked micro-barometer signals. Figure 7 shows the PMCC analysis of the intercepted waveform. At this increased distance, the lower frequencies arrive prior to the higher frequencies in a “chirp” consistent with the observations made by Farges [1] from 400km.

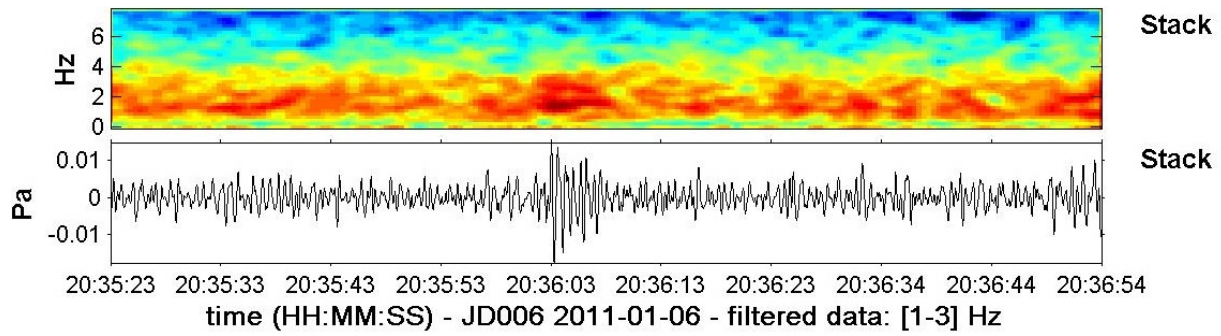


Figure 6: Pressure spectrum and stacked pressure pulse from the sprite in Figure 7

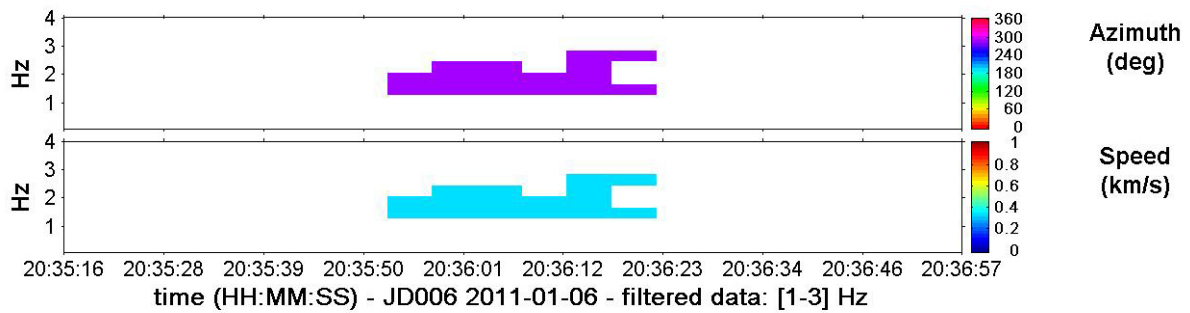


Figure 7: PMCC waveform analysis of the signal from a sprite on the night of 6 January, 2011

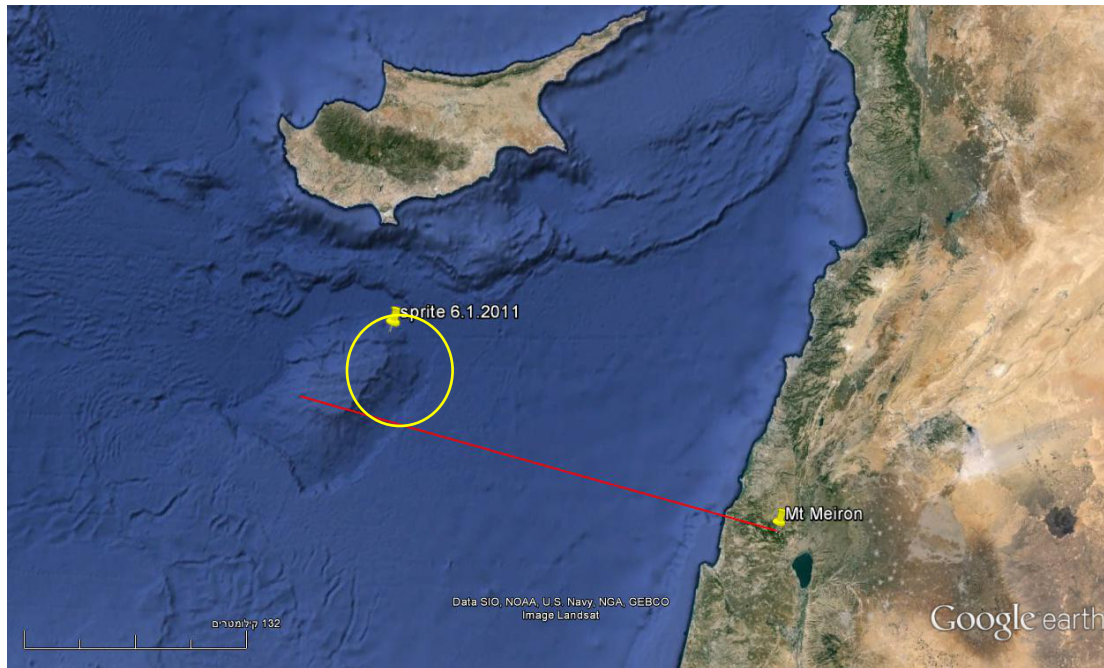
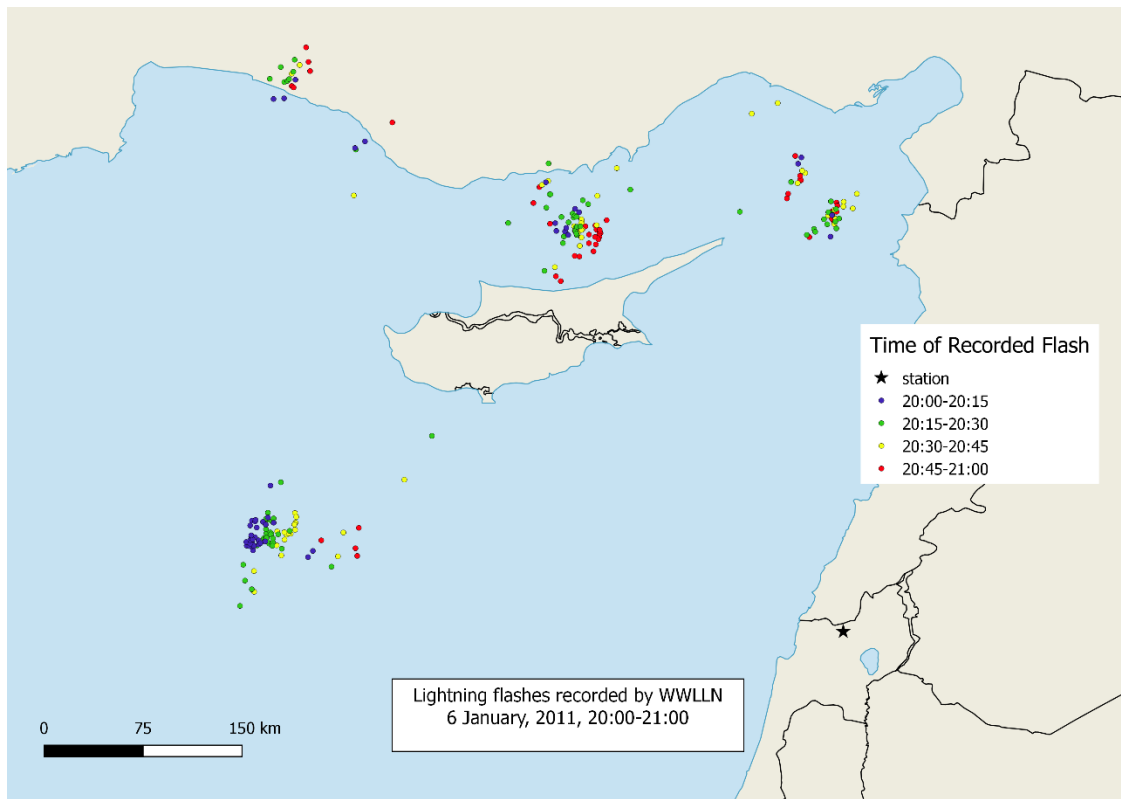


Figure 8: The location of the sprite in Figure 5, the back azimuth of the infrasound detection, and the oval in which the greatest number of rays originated.

673
674
675 Figure 8 shows the back-azimuth of the detected infrasound signal from this sprite, as well as the
676
677 predicted location of the sprite based on the ray tracing model. The two sprites at 20:19:05
678
679 provided the best fit, with the slightly later one being larger and therefore more likely. Once
680
681 again, the highest density of initial ray positions came from the area between the given center of
682
683 the image and the infrasound back-azimuth. When comparing that figure with Figure 9, which
684
685 shows the lightning activity detected by WWLLN in the period of time surrounding the sprite,
686
687 one can again see that there was intense lightning activity at the correct place at the correct time.
688
689



714
715 Figure 9: WWLLN flash detections from the time period surrounding the sprite detection. WWLLN
716
717 detected lightning flashes from the area of the infrasound detection during the correct time period. The
718
719 sprite occurred during the yellow interval.

722 Discussion and Conclusions

723
724
725

729
730
731 We have shown that the Meron infrasound array is capable of observing the infrasound signals
732 from sprites occurring in Eastern Mediterranean thunderstorms. Moreover, we have associated
733 the “inverted chirp” of a sprite at close range with a specific, photographed sprite, and confirmed
734 this observation using both electrical activity data and ray tracing technique.
735
736
737
738

739
740 While performing this study, we discovered three potential sources of uncertainty in our
741 observations: the large FOV of the sprite cameras, the fact that storms produce many sprites, not
742 all of which are imaged (because of dimness), and the slight lateral deviations in propagation
743 azimuth due to local winds. Error attributed to local winds is likely small, because of the
744 relatively short transit time of the wave to our detector arrays. Most of the time, there was little
745 difference between the sprite’s optical location and the infrasound back-azimuth. The next
746 potential source of error was the camera FOV. Although potentially up to seven degrees in
747 either horizontal direction, we found that the deviation was most of the time much less than this,
748 since the camera is pointed at the center of sprite-producing electrical activity in the first place.
749
750
751
752
753
754
755
756
757
758

759 Rather, what we found most often in our data were sprite-like signals missed by the cameras.
760
761

762 In some cases, two sprites may occur in a very short amount of time and from a very similar
763 location. In these cases, it may not be possible to tell which sprite produced the recorded
764 infrasound unless one sprite is markedly larger than the other. Furthermore, should both produce
765 detectable infrasound, the pressure pulse of the first may mask that of the second.
766
767
768
769
770

771 The literature makes it clear that it takes a big sprite or a close sprite to make a detectable
772 infrasound signal, and our results are very much in agreement with this. Most notably, we are
773 able to provide visual confirmation that close-range sprites cause the kind of inverted chirps seen
774 by Farges and Blanc [11]. In that paper, the authors lament that they were unable to provide
775
776
777
778
779
780
781
782
783
784

785
786
787 such visual confirmation because their interceptions came from azimuths not imaged by their
788
789 cameras.
790

791
792 Most of all, we verified that the Meron infrasound array is in excellent working order and able to
793
794 contribute to future observations of eastern Mediterranean sprites, especially during times of low
795
796 visibility when optical imaging is challenging.
797

798 799 800 801 **Acknowledgements**

802
803
804 This project was funded by a grant from the Israel Science Foundation No. 942/13. This project
805
806 was also generously supported by the European Science Foundation's Thunderstorm Effects on
807
808 the Atmosphere-Ionosphere System project (TEA-IS). The authors also wish to thank the entire
809
810 staff of the Israeli NDC and the ILAN science team for their data access and support.
811
812
813
814
815
816
817
818
819
820
821
822
823
824
825
826
827
828
829
830
831
832
833
834
835
836
837
838
839
840

841
842
843 **References**
844
845

- 846 [1] T. Farges, E. Blanc, a. Le Pichon, T. Neubert, and T. H. Allin, “Identification of
847
848 infrasound produced by sprites during the Sprite2003 campaign,” *Geophys. Res. Lett.*, vol.
849
850 32, no. 1, pp. 1–4, 2005.
851
852
- 853 [2] Y. Yair, C. Price, M. Ganot, E. Greenberg, R. Yaniv, B. Ziv, Y. Sherez, A. Devir, J. Bör,
854
855 and G. Sători, “Optical observations of transient luminous events associated with winter
856
857 thunderstorms near the coast of Israel,” *Atmos. Res.*, vol. 91, no. 2–4, pp. 529–537, Feb.
858
859 2009.
860
- 861 [3] S. a. Cummer, N. Jaugey, J. Li, W. a. Lyons, T. E. Nelson, and E. a. Gerken,
862
863 “Submillisecond imaging of sprite development and structure,” *Geophys. Res. Lett.*, vol.
864
865 33, no. 4, pp. 30–33, 2006.
866
867
868
- 869 [4] V. P. Pasko, U. S. Inan, and T. F. Bell, “Spatial structure of sprites,” *Geophys. Res. Lett.*,
870
871 vol. 25, no. 12, pp. 2123–2126, Jun. 1998.
872
873
- 874 [5] C. Price and B. Federmesser, “Lightning-rainfall relationships in Mediterranean winter
875
876 thunderstorms,” *Geophys. Res. Lett.*, vol. 33, no. 7, pp. 13–16, 2006.
877
878
- 879 [6] Y. Yair, Z. Levin, and O. Altaratz, “Lightning phenomenology in the Tel Aviv area from
880
881 1989 to 1996,” *J. Geophys. Res.*, vol. 103, no. D8, p. 9015, Apr. 1998.
882
883
- 884 [7] A.J.Bedard, Jr., W.A.Lyons, R.A.Armstrong, T.E.Nelson, B.Hill, and S. Gallagher
885
886 “A search for low-frequency atmospheric acoustic waves associated with sprites,
887
888 blue jets, elves, and storm electrical activity” AGU, 80(46), Fall Meeting (1999)
889
890
891
892
893
894
895
896

- 897
898
899 [8] L. Liskka and Y. Hobara, “Sprite-attributed infrasonic chirps-their detection, occurrence
900 and properties between 1994 and 2004,” *J. Atmos. Solar-Terrestrial Phys.*, vol. 68, no. 11,
901 pp. 1179–1188, 2006.
902
903
904
905
906 [9] V. P. Pasko, “Mechanism of lightning-associated infrasonic pulses from thunderclouds,”
907 *J. Geophys. Res. Atmos.*, vol. 114, no. 8, pp. 1–10, 2009.
908
909
910
911 [10] T. Farges and E. Blanc, “Characteristics of infrasound from lightning and sprites near
912 thunderstorm areas,” *J. Geophys. Res. Sp. Phys.*, vol. 115, no. 6, pp. 1–17, 2010.
913
914
915
916 [11] S. De Larquier and V. P. Pasko, “Mechanism of inverted-chirp infrasonic radiation from
917 sprites,” *Geophys. Res. Lett.*, vol. 37, no. 24, pp. 1–5, 2010.
918
919
920
921 [12] M. Ganot, Y. Yair, C. Price, B. Ziv, Y. Sherez, E. Greenberg, A. Devir, and R. Yaniv,
922 “First detection of transient luminous events associated with winter thunderstorms in the
923 eastern Mediterranean,” *Geophys. Res. Lett.*, vol. 34, no. 12, p. L12801, Jun. 2007.
924
925
926
927
928 [13] Y. Ben Horin, “Mount Meiron Infrasound array performance assessment,” *Tech. Report*,
929 *SNRC*, 2013.
930
931
932
933 [14] K. S. Virts, J. M. Wallace, M. L. Hutchins, and R. H. Holzworth, “Highlights of a new
934 ground-based, hourly global lightning climatology,” *Bull. Am. Meteorol. Soc.*, vol. 94, no.
935 9, pp. 1381–1391, 2013.
936
937
938
939
940 [15] R. L. Dowden, J. B. Brundell, and C. J. Rodger, “VLF lightning location by time of group
941 arrival (TOGA) at multiple sites,” *J. Atmos. Solar-Terrestrial Phys.*, vol. 64, no. 7, pp.
942 817–830, 2002.
943
944
945
946 [16] S. F. Abarca, K. L. Corbosiero, and T. J. Galarneau, “An evaluation of the Worldwide
947
948
949
950
951
952

- 953
954
955 Lightning Location Network (WWLLN) using the National Lightning Detection Network
956 (NLDN) as ground truth,” *J. Geophys. Res. Atmos.*, vol. 115, no. 18, pp. 1–11, 2010.
957
958
959
960 [17] C. J. Rodger, J. B. Brundell, R. L. Dowden, C. J. Rodger, J. B. Brundell, R. L. D.
961 Location, and V. L. F. W. Lightning, “Location accuracy of VLF World-Wide Lightning
962 Location (WWLL) network : Post-algorithm upgrade To cite this version : HAL Id : hal-
963 00317524 Annales Geophysicae Location accuracy of VLF World-Wide Lightning
964 Location (WWLL) network : Post-algorithm upgrade,” 2005.
965
966
967
968
969
970
971 [18] Y. B.-A. and E. A. Yair, Y., C. Price, D. Katzenelson, N. Rosenthal, L. Rubanenko, “Sprite
972 climatology in the Eastern Mediterranean region,” *Atmos. Res*, vol. 157, pp. 108–115,
973 2015.
974
975
976
977
978 [19] Y. Cansi, “An automatic seismic event processing for detection and location: The
979 P.M.C.C. Method,” *Geophys. Res. Lett.*, vol. 22, no. 9, pp. 1021–1024, May 1995.
980
981
982
983 [20] D. D. Sentman, E. M. Wescott, R. H. Picard, and J. R. Winick, “Simultaneous
984 observations of mesospheric gravity waves and sprites generated by a midwestern
985 thunderstorm,” 2003.
986
987
988
989
990 [21] C. L. da Silva and V. P. Pasko, “Infrasonic acoustic waves generated by fast air heating in
991 sprite cores,” *Geophys. Res. Lett.*, vol. 41, no. 5, pp. 1789–1795, Mar. 2014.
992
993
994
995 [22] V. P. Pasko and J. Snively, “Mechanism of infrasound radiation from sprites,” in *Eos*
996 *Transactions American Geophysical Union*, vol. 80, 2007.
997
998
999
1000 [23] G. M. Z. S. S. Abdullaev, *Chaos and dynamics of rays in waveguide media*. Gordon and
1001 Breach Science Publishers, 1993.
1002
1003
1004
1005
1006
1007
1008

- 1009
1010
1011 [24] J. X. Dessa, J. Virieux, and S. Lambotte, “Infrasound modeling in a spherical
1012 heterogeneous atmosphere,” *Geophys. Res. Lett.*, vol. 32, no. 12, pp. 1–5, 2005.
1013
1014
1015
1016 [25] D. Fee, R. Waxler, J. Assink, Y. Gitterman, J. Given, J. Coyne, P. Mialle, M. Garces, D.
1017 Drob, D. Kleinert, R. Hofstetter, and P. Grenard, “Overview of the 2009 and 2011
1018 Sayarim Infrasound Calibration Experiments,” *J. Geophys. Res. Atmos.*, vol. 118, no. 12,
1019 pp. 6122–6143, 2013.
1020
1021
1022
1023
1024
1025
1026
1027
1028
1029
1030
1031
1032
1033
1034
1035
1036
1037
1038
1039
1040
1041
1042
1043
1044
1045
1046
1047
1048
1049
1050
1051
1052
1053
1054
1055
1056
1057
1058
1059
1060
1061
1062
1063
1064

Conflict of Interests

The authors state that there are **no** conflicts of interest in publishing this manuscript, whether between authors, institutions or funding agencies.